Nonlinear Analysis of Reinforced Concrete as a Minimization Problem, by a Finite Element Representation of the Stress Field

Analyse non-linéaire du béton armé comme problème varationnel, pour les éléments finis qui définissent le champ des contraintes.

Nichtlineare Berechnung von Stahlbeton als Minimierungsproblem, mit Finite-Elemente-Darstellung des Spannungsfeldes

GIANFRANCO VALENTE
Prof. Ing.
University of Rome
Rome, Italy

SUMMARY

In previously published papers [4], [7], [8], [9], the approach to the limit analysis of reinforced concrete bodies was formulated as a minimax problem, whose solution could be achieved by means of an appropriate algorithm based on the discretization of the structure into finite elements. This algorithm was implemented in a computer program including an incremental method, where the steps amplitude is defined by crack development. In this paper, the problems connected with the numerical performance of that procedure are taken into account. Finally, the experimental data on concrete rings for determining tensile strength of concrete obtained by Malhotra [5] are compared with numerical results of the proposed method.

RÉSUMÉ

Dans les publications précédentes [4], [7], [8], [9], l'approche des états-limites de béton armé était formulée sous forme d'un problème variationnel, dont la solution pouvait être approximée par éléments finis. La discrétisation dans le temps était definie par le développement successif des fissures. Cette publication-ci prend la performance numérique de cette procédure sous la loupe. Ensuite la méthode proposée est appliquée à la détermination de la résistance à la traction de béton non-armé. Les résultats numériques correspondent aux données expérimentales de Malhotra [5].

ZUSAMMENFASSUNG

Grenztragfähigkeitsanalyse von Stahlbeton wurde als Minimaxproblem behandelt auf der Grundlage finiter Elemente. Diese Methode wurde in ein Computerprogramm implementiert, wobei die Inkremente durch die Rissentwicklung bestimmt sind. In diesem Bericht wird die numerische Behandlung beschrieben und auf das Beispiel der Betonringzugprüfung angewandt.

1. SYMBOLS

They are as follows:

NC number of concrete nodes,
NS number of steel nodes,
NEC number of concrete elements,
NES number of steel elements,
NVS number of aligned bars couples,
KK total number of equilibrium equations,
NN number of linearly independent equations,
number of kynematic independent parameters,
LL number of static independent parameters,
MM total number of static parameters,
NF total number of failure functions.

2. INTRODUCTION

The author have developed a finite element method for finding lower bounds on the limit load for reinforced concrete with perfectly plastic steel and perfectly brittle concrete. Let the two dimensional domain R be subdivided into elements triangular for concrete and linear for steel bars.
Stress and velocity components relevant to the problem under consideration are assumed to have linear distribution within each element, and to be continuous across the elements boundaries. In this way a family of stress fields is considered, whose generic member is identified by the values that the stress components assume at the nodal points. The bound stresses between steel and concrete and the dowel effect are taken into account. Let the stress values be collected in a vector $\underset{\sim}{\sigma}$.
Vector σ has MM = 3 NC + 5 NES components
(plane stress components σ_x, σ_y and τ_{xy} for concrete nodes; normal, shear and bond stresses σ_i, σ_j, τ_i, τ_j and τ_d for steel bars).
A family of velocity fields is also considered whose generic member is identified by the values of the velocity components at the nodal point; values collected in a vector $\underset{\sim}{u}$. The total number of equilibrium equations is KK = 2 NC + NVS + NES and the dimension of vector u is NN = KK - NV.
Now a somewhat restricted equilibrium condition is imposed to the stress fields previously defined, by means of the virtual work theorem, taking as a virtual kinematic field any member of the family of velocity fields previously defined, together with the strain rate field kinematically consistent with it.
The virtual work equation may then be written as

$$\underset{\sim}{u}^T \underset{\sim}{Q}\, \underset{\sim}{\sigma} - \rho\, \underset{\sim}{u}^T \underset{\sim}{p}_2 = 0 \qquad (1)$$

The first term in Eq. (1) is the internal virtual work, $\underset{\sim}{Q}$ being the equilibrium matrix, assembled as shown in Fig. 1, depending upon the assumed stress and velocity distribution. The second and the third terms are the external virtual work due to external load p_1 and to prestressing loads $\underset{\sim}{p}_2$, ρ is the multiplier of external load $\underset{\sim}{p}_1$ alone.

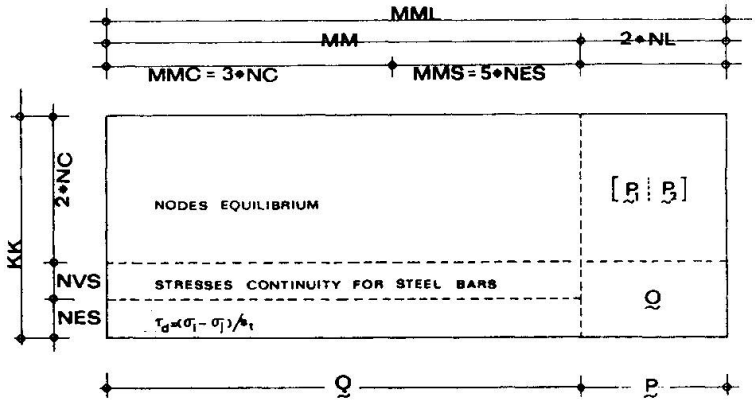

Fig. 1 - Matrix $\underset{\sim}{Q}$

Obviously, Eqs (1) are necessary, but not suffient conditions for equilibrium, because all the virtual kinematic filed have not been considered, but only a subset of them. Now let it be consider checking the yield condition (with analytical representation of concrete experimental data by Kupfer, Hlsdorf and Rüsch [3], von Mises criterium and comparison with maximum bond strength for steel)

$$f_i = \varphi_i(\rho\underset{\sim}{\sigma}) \leqslant 1, \ (i = 1, .., NF), \ (NF = NC + 3 \cdot NES) \tag{2}$$

the limit analysis problem is solved by the unconstrained minimization of the nonstrictly convex function

$$\Phi(\underset{\sim}{\sigma}^*_K) = \max_i \left[f_i(\underset{\sim}{\sigma}^*_K)\right] \quad (k = 1, .., LL) \tag{3}$$

where $\sigma^*$are the LL = MM - NN undependent parameters. The irregular function Φ is replaced by a sequence of every-where regular approximation of this function:

$$\varphi_\alpha = \left[\frac{1}{NF} \quad \Sigma_i \ \varphi_i^\alpha\right]^{1/\alpha} \tag{4}$$

In this paper, the numerical problems are examined more accurately then in previous papers [7], [8], [9].

3. EQUILIBRIUM MATRIX FOR A STEEL ELEMENT

It may be obtained by taking into account a rectangular element composite with two triangular elements. If the equilibrium matrices for triangular elements having linear distribution for stress and strain fields, and if a side of this rectangular element approaches to zero, then the equilibrium matrix for a linear element is obtained for the nodal stresses σ_i, σ_j, τ_i and τ_j.

4. FREE AND DEPENDENT PARAMETERS

The matrix $\underset{\sim}{Q}$ has zero rows, for the boundary kinematic condition, and since the problem:

$$\underset{\sim}{Q}\ \underset{\sim}{\sigma} = \rho\ \underset{\sim}{p}_1 + \underset{\sim}{p}_2 \tag{3}$$

has solutions, such general solution can be obtained in the form

$$\underset{\sim}{\sigma} = \underset{\sim}{\sigma}^*_o + \underset{\sim}{Q}^*\ \underset{\sim}{\sigma}^* \tag{4}$$

where

$$\underset{\sim}{\sigma}^*_o = \underset{\sim}{\rho}\ \sigma^*_{o2} + \underset{\sim}{\sigma}^*_{o2}$$

where $\underset{\sim}{\sigma}^*_o$ is a particular solution, $\underset{\sim}{\sigma}^*$ is linearly independent vector and $\underset{\sim}{Q}^*$ are arbitrary parameters.

The program is able to find the rank, designate the rows and the columns which provide a nonsingular square submatrix of that rank, and give the value of the determinant of that submatrix by using the Gaussian elimination process shown by Ralston [2].

When any of the divisors q_{ii} (diagonal element in Q^*_D) is small in magnitude compared with other elements q_{ij} of same matrix, then a serious round off error may be incurred.

To avoid these divisions, a technique called *positioning for size* is used. At the i-th stage of calculation (i = 1, ..., NN) it consists of the following:

- rows are interchanged to get nonzero rows in the first NN positions,
- columns are interchanged in order to locate that element q_{ii} of greatest absolute magnitude.
- then the elements in the i-th row are calculated by the so-called back substitution.
- the rows and columns interchangings are memorized in two vectors IROW and ICOL.

Finally, the matrix assembled as in Fig. 3 is obtained

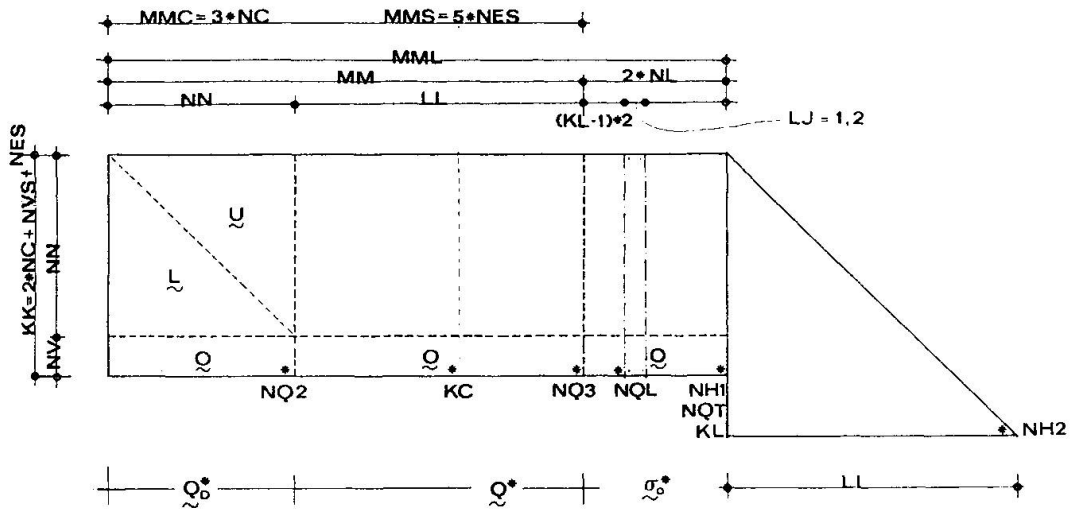

Fig. 2 - Resolutive matrix Q

where, NN is the rank of $\underset{\sim}{Q}^{*}_{D} = \underset{\sim}{L}\ \underset{\sim}{U}$ and of the dependent parameters, LL = MM - NN is the free parameters number. The triangular matrix at the right side of Fig. 3 represents the gradient coefficients for the free parameters and are computed by partial derivatives of plastic power $\Phi(\underset{\sim}{\sigma}^{*})$.

5. TESTS CHECKING

The tests (g), (i), (j) and (l) in the flow-chart of Fig. 2 are a very tiklish and important elements of the computer program.
The test (l) in the loop 1 permits to find the new cracks pattern for the stresses field which minimizes the plastic power Φ.
Let the following terms be considered:

$$\varepsilon_1 = | 1 - \varphi_{max} |, \quad \varphi_{max} = \max_i \varphi_i \ (i = 1, \ldots, NC) \tag{6}$$

$$\varepsilon_2 = | 1 - \varphi^{+} | \tag{7}$$

$$\varepsilon = \max (\varepsilon_1, \varepsilon_2) \tag{8}$$

where φ^{+} is the maximum value of function φ computed between the not cracked nodes with positive value of the first principal stress.
To take into account the value ε_2 is very important because only the cracking in the nodes subjected to tension may produce substantial variation of the stress

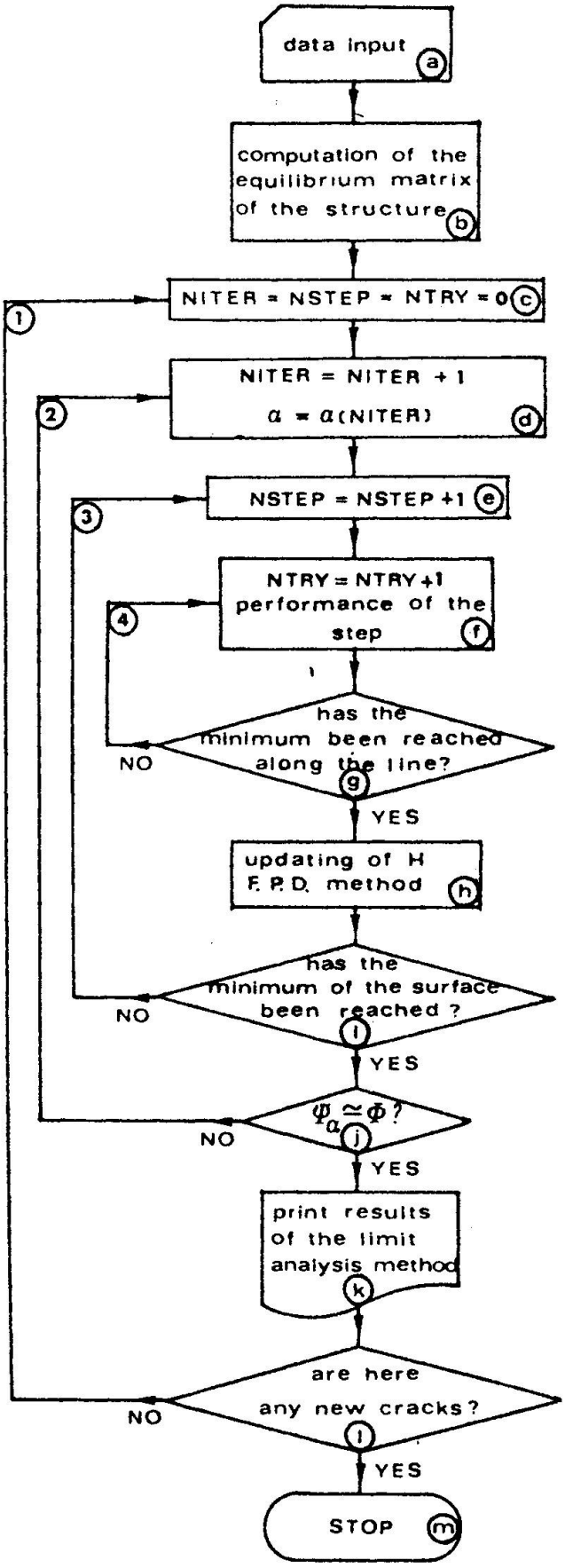

FIG. 3. - Flow-chart of the process; cycles ② , ③ and ④ constitute logical outline of limit analysis by nonlinear programming

field.
From a computational viewpoint, a new crack in a node produces a reduction of the failure domain only in the tension-tension or tension-compression zones. Then, if the point of the stress state was in this zone in the neigh-bouring of the yield line, after the cracking it will shift brusquely causing a substantial change in the whole stress field for the equilibrium of the same.
The value ε is used to calculate the following prescribed small positive value $\bar{\varepsilon}$ depending on the ratio between the two principal stresses

$$\bar{\varepsilon} = c_1 \varepsilon, \qquad \text{for } (\sigma_2 + 3\sigma_1) \leqslant 0 \tag{9}$$

$$\bar{\varepsilon} = c_2 + \frac{c_2 - c_1}{3} \frac{\sigma_2}{\sigma_1} \varepsilon, \qquad \text{for } \sigma_2 > 0,\ \sigma_2 \leqslant 0 \tag{10}$$

$$\bar{\varepsilon} = c_2 \varepsilon \qquad \text{for } \sigma_1,\ \sigma_2 \geqslant 0 \tag{11}$$

A node will became cracked if it is:

$$\varphi \geqslant 1 - \bar{\varepsilon} \tag{12}$$

It agrees to assume for c_1, c_2 the following values

$$c_1 = 1{,}5 \div 2{,}0\ ; \qquad c_2 = 3 \div 6 \tag{13}$$

In such a way, the biaxial tension stress states are penalized greatly than the biaxial compression stress states with linear interpolation for middle states. Smaller values will be selected for c_1 and c_2 parameters if it is deemed to follow the cracking phenomenon with greater accurancy; obviously, this behaves much more steps in the evolutive process.
The process is illustrated in the following Fig. 4

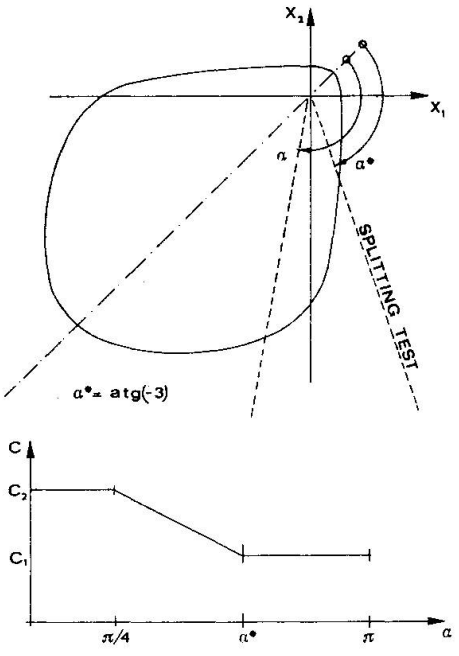

Fig. 4 - Computation of the parameter c (σ_1, σ_2)

The test (h) for the loop 2 checks that two surface ψ_α and Φ are enough close between themselves. When the minimum on the surface ψ_α has been ottained, the collapse multiplier for the node i-th having $\varphi_{max} = \max \varphi_k$ (K = 1, .., NC) is computed. The failure function is a fourth order polinominial and the condition:

$$\varphi_i \ (\rho_i \ \sigma) = 1 \qquad (14)$$

leads to four roots. Related to the Fig. 5 two kind of solution are possible:
- for the stress state represented by the point A, four real roots are obtained,
- for the stress state B, two real roots and two complex roots are obtained;
the true solution is the smaller real positive root (like points A_2 and B_1).

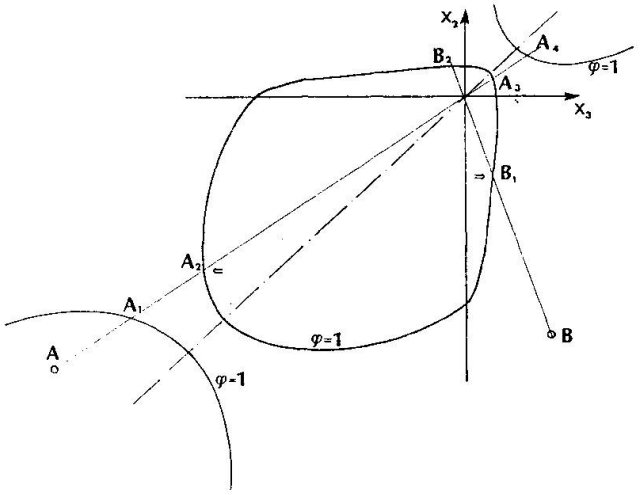

Fig. 5 - Solution of the fourth order polinomial

The error on this value of ρ_α is computed by the aim of the following Fig. 6.

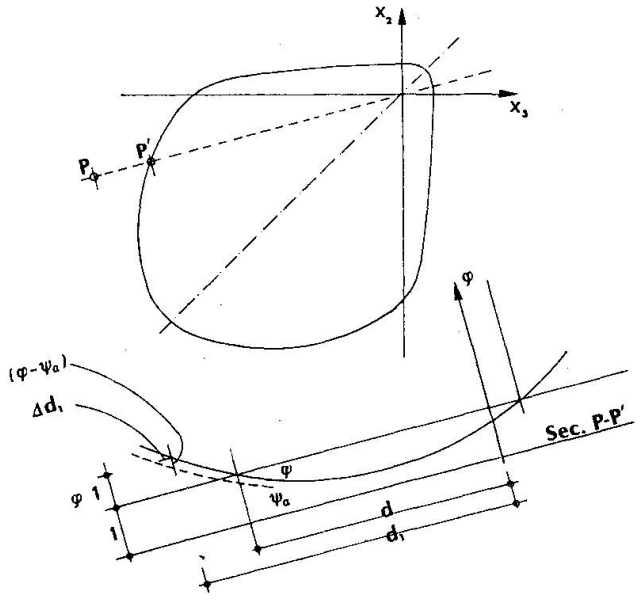

Fig. 6 - Error on the collapse multiplier computation

This error is deduced by the following relationships:

$$\rho_\alpha = \frac{d}{d_1} \quad f(d_i) \tag{15}$$

$$\Delta\rho_\alpha = \frac{df}{dd_1} \quad \Delta d_1 = \frac{d}{d_1^2} \quad \Delta d_1 \tag{16}$$

$$\Delta d_1 = (\varphi - \psi_\alpha) \ (d_1 - d)/(\varphi - 1) \tag{17}$$

$$\Delta\rho_\alpha = \rho_\alpha \ (\varphi - \psi_\alpha) \ (1 - \rho_\alpha)/(\varphi - 1) \tag{18}$$

The test (h) consists in the checking:

$$\Delta\rho_\alpha/\rho_\alpha \leqslant \varepsilon_{tol} \tag{19}$$

Where ε_{tol} is a prescribed small positive quantity. The test (i) in the loop 3 checks that the minimum position of the surface ψ_α has been ottained, this happen when between the initial and final values ψ_o, ψ_1 is

$$2 \ (\psi_o - \psi_1)/(\psi_o + \psi_1) \leqslant s_{lim} \tag{20}$$

This condition, in spite of its simplicity, displays itself to like better than other more complex, like gradient modulus.
The test (g) in the loop 4 checks that the minimum of the line has been attained; it is admitted that this test is satisfied when a value ψ_α less then all the preceding values on the line is obtained. The loops 2 , 3 and 4 are better shown by the paper of Fletcher and Powell [1]
The value S_{lim} is a prescribed small quantity; for $\varepsilon_{tol} = 10^{-2} \div 10^{-3}$, the better computational value was:

$$S_{lim} = 10^{-6} \div 10^{-7} \tag{21}$$

6. RUNNING TIME FOR THE EVOLUTIVE PROCESS

This computer time necessary to the program running may be subdivided into three parts:
- data memorization,
- computation of equilibrium and non singular matrices $\underset{\sim}{Q}$ and $[\, Q_D^* \quad Q^* \ \sigma_o^* \,]$ respectively
- minimization times for each step.

The first two computer times represent a derisive part of the total time, then the third part is the more important time.
In the following Fig. 7 the computer times for a single minimization in absence of cracked nodes is represented.
This time is placed near the relationship:

$$t = 10^{-2} \ (1 + 75 \ \alpha) \ LL \quad NC \tag{22}$$

where $\varepsilon_{tol} = 10^{-\alpha}$ is the prescribed small value for ρ_α in the minimization.
If cracked node exist, and if NCl is the number of the nodes having the tensile first principal stress before the cracking, the minimization time is greather

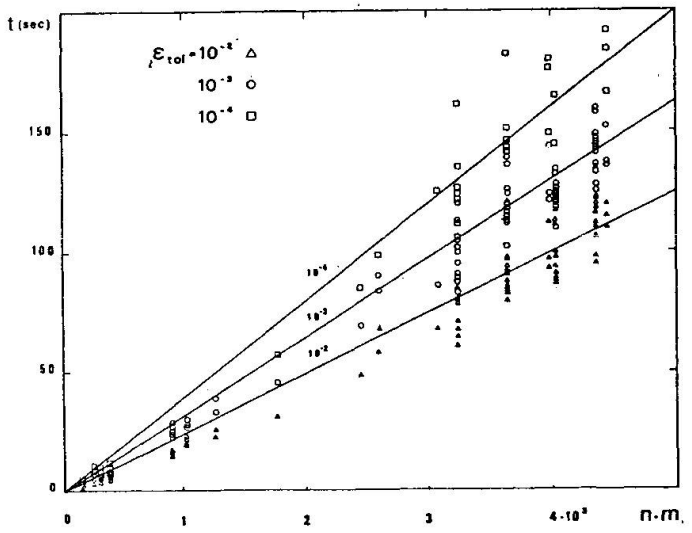

Fig. 7 - Minimization time in absence of cracked nodes.

then the aforementioned time according to the relationship:

$$t = 10^{-2}(1. + .75\ \alpha)\ LL\ \ NC(1. + 3.5\ NC1/NC) \qquad (23)$$

These relationships are obtained:

- by the numerous computer solutions of analogous problems for bodies with material according to Von Mises yield criterium,
- by the numerical solution of the famous beam tested by Bresler and Scordelis and of the concrete ring specimen numerical solved.

These computer times are related to UNIVAC 1100.

7. STORAGE USED

By the aforementioned notations this computer storage is defined by the following relationship:

$$55 \cdot NC + 4 \cdot NEC + 37 \cdot NES + 5 \cdot LL + 22 \cdot NL + 8 \cdot NC \cdot NL + (2 \cdot NC + 2 \cdot NS)\ (3 \cdot NC + 4 \cdot NES + 2 \cdot NL) + LL^2/2 + 2 \cdot NF + 20.000 \qquad (22)$$

8. NUMERICAL EXAMPLE

In the Malhota paper [5] regression analysis were carried out to establish correlation between inside diameter ring tensile strength and 4x8 in. (10x20 cm) cy-

linder compressive strength. All the reported data had been carried out using two kind of specimens like in following Table 1:

Table 1 - Ring specimens data

Specimen N.	Inside diameter	high	wide	P_{iu}	σ_t	ε
1	6 in (15cm)	1½ in. (3.8cm)	1½ in (3.8cm)	21.040	54.704	9.408
2	12 in (30cm)	3 in (7.5cm)	3 in (7.5cm)	20.960	54.496	8.992
				kg/cm^2	kg/cm^2	%

The Author found the following relationship:

$$Y = .063X + 17.5 \text{ kg/cm}^2$$

where Y and X are the inside diameter ring tensile strength and the cilinder compressive strength, respectively. Besides this the Author says that the tensile stresses in the ring section vary linearly from a maximum of 2.6 P_i at the internal periphery to 1.6 P_i at the outside periphery, where P_i is the applyed hydrostatic pressure.

In the subsequent discussion, Pandit [6] says that none of the existing methods for the determination of the tensile strength of concrete campare favorably as regard reproducibility or reliability with the compression test.

The aforementioned specimens have been represented by the finite element mesh in the following Fig. 8.

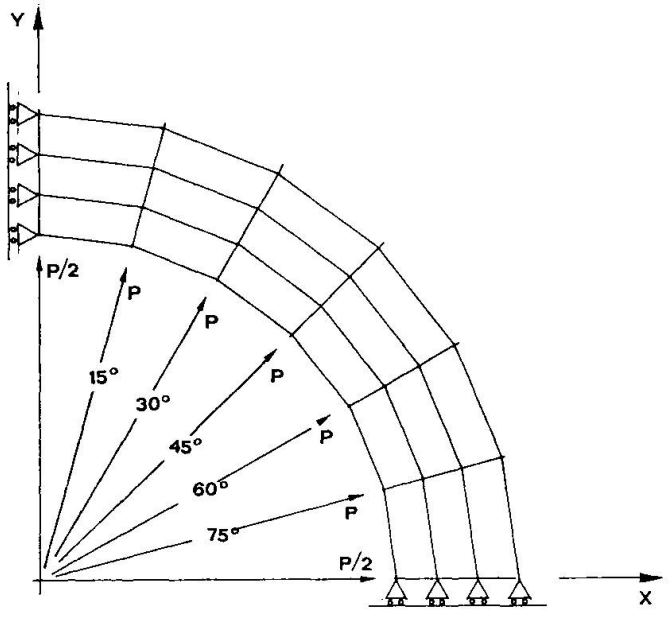

Fig. 8 - Finite element mesh

For these specimens the tensile and compressive strengths were 50. and 500. kg/cm^2 respectively and the ultimate hydrostatic pressures were those shown in Table 1. By admitting that the maximum tensile stress in the ring section is 2.6 P_{iu} at the inside periphery, there is the tensile stresses in the Table 1.

REFERENCES

1. FLETCHER, R. - POWELL, M.J.D.: "A rapidly convergent descent method for minimization", computer Jrn., Vol. 6, 1963.

2. RALSTON, A.: "A first course in numerical analysis", Mc Graw Hill, New York 1965, Chapter 9 § 3.

3. KUPFER, H. - HILSDORF, H. - RÜSCH, H: "Behavior of concrete under biaxial stresses,", Proceedings ACI, Vol. 66, August 1969.

4. CASCIARO, R. - DI CARLO, A. - VALENTE, G.: Discussion on "Plane stress limit analysis by finite elements" by T. Belytschko and P. Hodge jr., Dec. 1970, Proc. ASCE, EM5 1971.

5. MALHOTRA, V.M.: "Concrete rings for determining tensile strength of concrete", ACI jrn., april 1970.

6. PANDIT, G.S. - Discussion of paper [4], ACI jrn., october 1970.

7. VALENTE, G.: "Nonlinear analysis of reinforced concrete by finite elements", Istituto di Scienza delle Costruzioni, Facoltà di Ingegneria, ROMA, paer n. II-185, November 1976.

8. VALENTE, G.: "Nonlinear analysis of prestressed reactor pressure vessels", 4th SMiRT Conference, San Francisco, California, U.S.A., August 1977.

9. VALENTE, G.: "Ultimate criteria of concrete under bi-axial loading", 5th SMiRT Conference, Berlin, Germany, August 1979.